Closed-loop tracking of amplitude and frequency in a mode-localized resonant MEMS sensor

Milind Pandit, Chun Zhao, Guillermo Sobreviela, Aref Mustafazade and Ashwin A Seshia
Nanoscience Centre, Department of Engineering, University of Cambridge,
11 JJ Thomson Avenue , Cambridge CB3 0FF

***Abstract*—In this paper, the amplitude and frequency stability of a mode-localized sensor are characterized in a closed loop setup. The system describes an absolute amplitude ratio sensitivity of 5250 to stiffness perturbations in linear operation. A stability of 432ppm at 500s integration time is observed for amplitude ratio measurements. A resolution of 85ppb corresponding to normalised stiffness perturbations in amplitude ratio measurements is thus demonstrated at 500s integration time. Comparisons to frequency shift sensing within the same device shows that amplitude ratio sensing provides higher accuracies for long term measurements due to intrinsic common mode rejection properties in a mode-localized system.**

I. Introduction

Mode localization in a configuration of Weakly Coupled Resonators (WCRs) have been shown to provide orders of magnitude higher sensitivity in Amplitude Ratio (AR) measurements as compared to conventional single resonator frequency shift measurements [1] [2]. The intrinsic common mode rejection of parametric noise in the amplitude ratio has been credited for its use in long term measurements as a sensor [3] [4] [5].

However, until recently, measurements of the resolution of a mode localised resonant sensor have all been characterised in an open loop configuration, where the resolution is significantly limited by the swept frequency network analyzer measurements. By measuring the minimum observable shift in amplitude ratio through a network analyzer, the resolution of the amplitude ratio of a coupled 2-DOF system was shown to be 0.0096 [6]. Using a similar approach, an open loop experiment on a mode localised accelerometer previously demonstrated a resolution of $619\mu g$ [7].

The oscillator system is adapted from the preliminary designs of the direct feedback oscillator for WCRs that have been shown previously through theoretical calculation and experimental validation[8] [9]. Although, an oscillator design was presented in this work [8], no further stability or resolutions were measured to fully establish the advantages of amplitude ratio measurements over conventional frequency shift measurements.

In this work, the stability, sensitivity and resolution of a prototype mode-localised sensor has been successfully characterized in a closed loop configuration. The paper also compares the resolution of the frequency shift and amplitude ratio as output metrics over a range of integration times, showing an improvement of up to 10x when using amplitude ratio as the readout metric over long integration times ($\tau > 500s$).

II. Experiment

A. Device Description

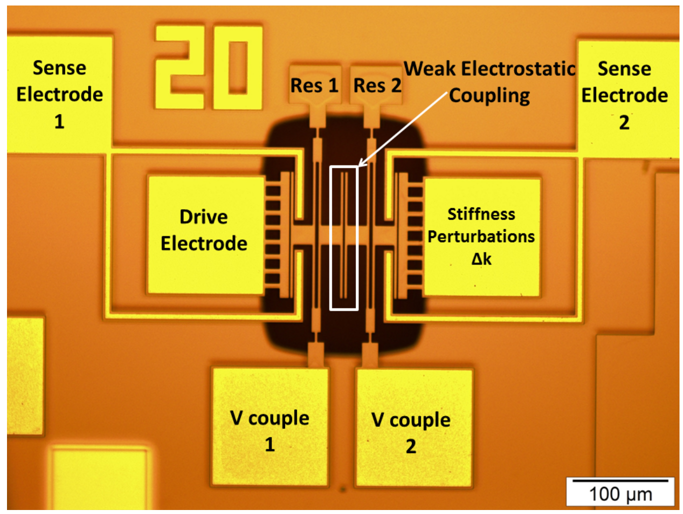

Fig. 1: Optical Micrograph of the device.

Two identical, coupled double ended tuning fork (DETF) resonators were used for this experiment. An optical micrograph of the device is shown in Fig. 1. The structural parameters of the device are provided in Table I. The device was fabricated by MEMSCAP Inc. using SOIMUMPS, a commercial process that uses silicon-on-insulator (SOI) wafers.

TABLE I: Device Parameters

Parameter	Dimensions
Beam Length	350 μm
Beam Width	6 μm
Electrode Length	260 μm
Electrode Width	6 μm
Device Layer Thickness	25 μm
Proof Mass (2 for each DETF)	40 μm $\times$ 40 μm
Electrode Gaps	2 μm

B. Measurement setup

All the experiments were conducted in a custom vacuum chamber at a pressure of 10mTorr without any temperature regulation in the chamber. The two resonators are weakly coupled by an electrostatic spring created by applying a voltage difference across an air gap electrode arrangement situated between the resonators. The drive electrode is used to drive resonator 1 with a combination of a DC polarization voltage and an AC excitation voltage. The two sense electrodes are biased at the same sense DC voltage and are used to sense the amplitude of vibration of both the resonators. The perturbation electrode is used to apply a DC voltage to introduce a negative stiffness perturbations on resonator 2 for characterization of device sensitivity. The loop is closed using the output current of resonator 1 that is first converted to a voltage through a Transimpedance Amplifier (TIA), then passed through a soft limiter for amplitude control and finally through phase shifters to satisfy the Barkhausen criteria. The experimental setup including the oscillator topology is illustrated in Fig. 2.

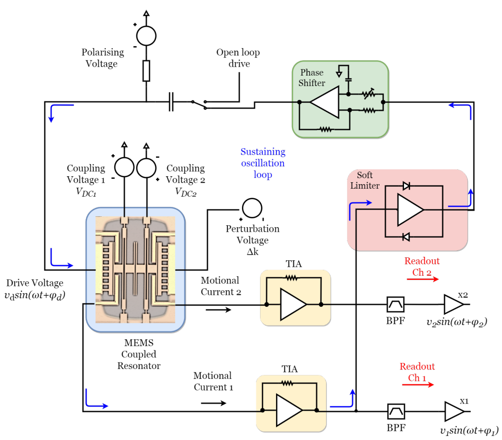

Fig. 2: Experimental Setup.

III. Results and Discussion

A. Stability Analysis

For stability analysis, the coupling voltage was set to 5V to achieve high sensitivity while ensuring that no modal overlap was observed. Furthermore, the resonators were biased to have an amplitude ratio of 10 based on an analysis of the operating range[10]. The loop was then closed in the anti-phase mode and the amplitudes of the respective resonators and the frequencies were measured for 16 hours in order to obtain their long-term stabilities. The stabilities of the frequency and amplitude ratio were characterized by the normalized Allan Deviation and presented for relative comparison in Fig. 3. A best stability of 432ppm in amplitude ratio was observed at $\tau = 500s$ while the frequency stability of 0.6mHz was achieved at $\tau = 0.2s$.

B. Sensitivity Analysis

Next, a sensitivity experiment was performed by applying stiffness perturbations on Resonator 2 while measuring the shift in amplitude ratio as well as frequency. The results are shown in Fig. 4. The results of the closed loop sensitivities of the two resonator amplitudes, the amplitude ratio and the frequency are compared to their open loop counterparts. Due to biasing the system away from the *veering zone*, the amplitude of resonator 1 (X_1) remains relatively constant while that of resonator 2 (X_2) changes with stiffness perturbations. Consequently, there is a a linear shift in amplitude ratio with the application of stiffness perturbations. Thus the amplitude ratio sensitivity to stiffness perturbations can be derived as:

$$S_{AR} = \frac{\partial AR}{\partial(\Delta k/k)} = -5250/(\Delta k/k) \tag{1}$$

The operating region of the oscillator is limited to the anti-phase mode where the modal frequency is insensitive to stiffness perturbations. Therefore, the frequency sensitivity presented in Fig. 4(d), where the closed loop frequency changes by only 2 Hz over the range of the stiffness perturbations, does not represent the maximum sensitivity achieved with frequency shift sensing in this device. In this particular operating region, the in-phase mode has the maximum frequency sensitivity. Due to the symmetry of in-phase mode and anti-phase mode, it is assumed that the frequency stability of in-phase mode is

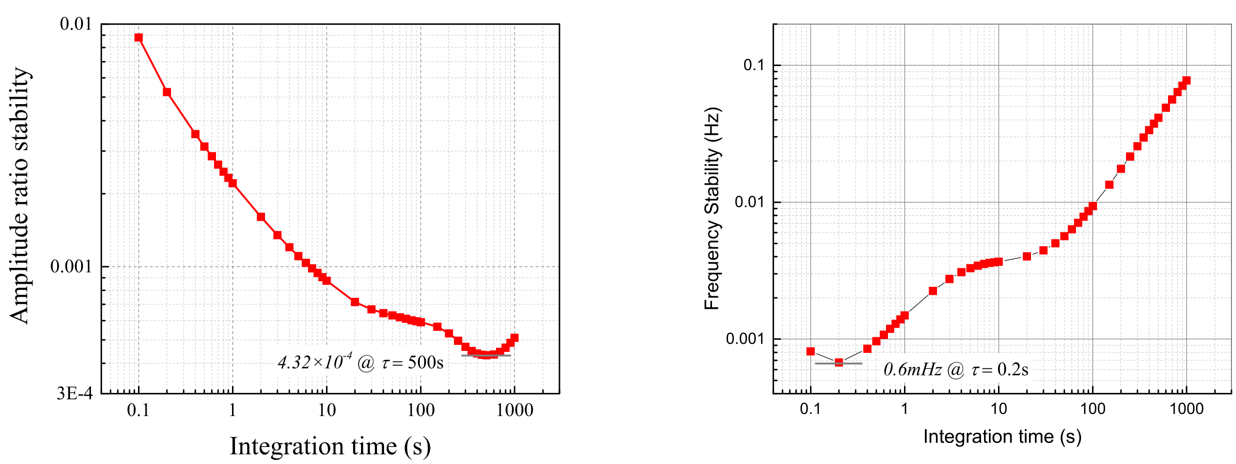

(a) (b)

Fig. 3: Stability of the amplitude ratio (a), and frequency (b) shown in terms of modified Allan deviation plots

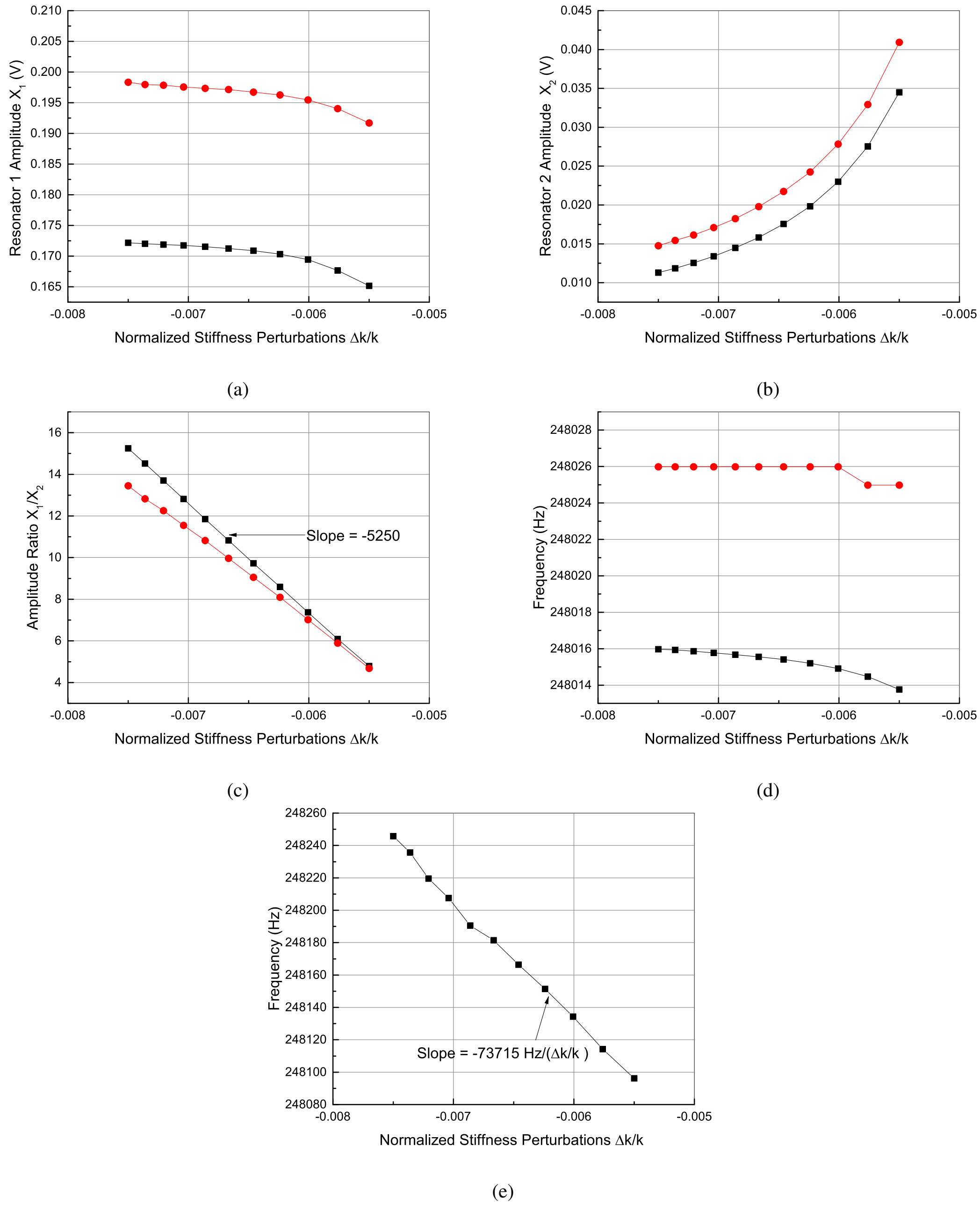

Fig. 4: Sensitivity of amplitude of resonator 1 (a) and resonator 2 (b), amplitude ratio (c), and frequency (d) in open loop (Red) and closed loop (Black) configuration .

similar to the anti-phase mode. To achieve the highest input referred resolution for the frequency shift sensitivity, frequency shifts in the in-phase mode, as shown in Fig. 4(e) are used [9]. With these two assumptions, the open loop frequency sensitivity of in-phase mode can be used as the approximate frequency sensitivity of the device. The sensitivity of the frequency shift output is found to be:

$$S_f = \frac{\partial f}{\partial(\Delta k/k)} = 73715 Hz/(\Delta k/k) \tag{2}$$

C. Input-referred Stability

Using the stability and the sensitivity calculated previously, the input-referred stability can be estimated for both amplitude ratio output and frequency shift output from the same device. The input referred stability signifies the minimum normalized perturbation $\langle \frac{\Delta k}{k} \rangle$ that can be sensed by the mode localized system. This can be calculated for amplitude ratio and frequency as follows:

$$\langle \frac{\Delta k}{k} \rangle_{AR} = \frac{\langle AR \rangle}{S_{AR}} \tag{3}$$

$$\langle\frac{\Delta k}{k}\rangle_f = \frac{\langle f\rangle}{S_f} \tag{4}$$

Equation 3 and Equation 4 are used to create the input-referred resolution curves for both amplitude ratio and frequency. These are superimposed upon each other to compare their input-referred stability at a range of integration times ($0.1s \leq \tau \leq 1000s$) in Fig. 5.

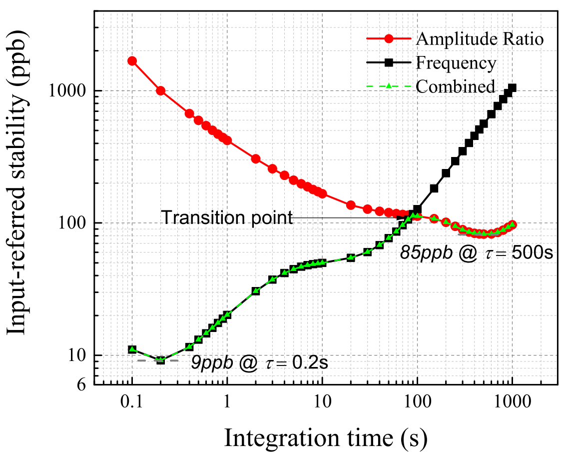

Fig. 5: Input-referred Resolution of frequency shift and amplitude ratio output

A minimum of 9ppb is estimated in the input-referred frequency stability at $\tau = 0.2s$ while a minimum of 85ppb is achieved in the input-referred amplitude ratio stability at $\tau = 500s$. The two curves intersect at $\tau \approx 100s$ after which, the resolution of amplitude ratio sensing is better than that of frequency shift sensing.

The results show that for short integration times (below 100s), frequency shift sensing provides a better measurement resolution. However, for longer integration times, amplitude ratio sensing allows for improved resolution due to the absence of common mode random variations, i.e. first order temperature dependent drifts, that are predominant in frequency shift sensing at larger integration times. The results thus demonstrate the potential benefits of using amplitude ratio shift sensing for applications that require high resolution for long term measurements. Additionally, combining both measurements within a single device could allow for both short-term and long duration high-resolution measurements to be conducted within the same device. Further improvements in amplitude-based readout techniques to reduce the impact of interface circuit noise will also enable measurements requiring both very high resolution and high stability to be conducted within the same MEMS device.

IV. Conclusion and Future Work

This work presents the first characterization of the input-referred resolution for both amplitude ratio and frequency shift output of the mode localized sensor operated in a closed loop setup. The results show that the input-referred stability for frequency shift sensing in the mode localized sensor is better at lower integration times while that of the amplitude ratio sensing is better at higher integration times. This behaviour is attributed to the rejection of common mode variations in amplitude ratio sensing that is predominantly present in frequency shift sensing.

This work also demonstrates the potential practical benefits of the amplitude ratio sensing over the conventional frequency shift sensing. However, there are many parameters that affect the stability of the measured amplitude and those need to be studied thoroughly to improve the stability of the system in both short and long integration times. Studies are being conducted currently to better understand the factors limiting the resolution of the amplitude ratio with the aim to improve the resolution of mode-localized sensing.

V. Acknowledgement

This work is supported by funding from Innovate UK and Natural Environment Research Council.

References

[1] P. Thiruvenkatanathan, J. Yan, J. Woodhouse, and A. A. Seshia,, "Enhancing Parametric Sensitivity in Electrically Coupled MEMS Resonators," *J. Microelectromechanical Syst.*, vol. 18. no. 5, pp. 1077-1086, Oct. 2009

[2] C. Zhao, G. .S Wood, J. Xie, H. Chang, S. H. Pu and M. Kraft, "Comparative study of different output metrics for a three weakly coupled resonator sensor," in *J. Microelectromechanical Syst.*, vol. 25, no. 4, pp. 626-636, 2016.

[3] P. Thiruvenkatanathan, J. Yan, and A. A. Seshia, "Differential amplification of structural perturbations in weakly coupled MEMS resonators," *IEEE Trans. Ultrason. Ferroelectr. Freq. Control*, vol. 57. no. 3,pp. 690-697, Mar. 2009

[4] M. Spletzer, A. Raman, A. Q. Wu, X. Xu, and R. Reifenberger, "Ultrasensitive mass sensing using mode localization in coupled microcantilevers," *Appl. Phys. Lett.*, vol. 88. no. 25,p.254102, Nov. 2015

[5] P. Thiruvenkatanathan, and A. A. Seshia,, "Mode-Localized Displacement Sensing," *J. Microelectromechanical Syst.*, vol. 21. no. 5, pp. 1016-1018, Oct. 2012

[6] P. Thiruvenkatanathan, J. Woodhouse, J. Yan, and A. A. Seshia, "Limits to mode-localized sensing using micro- and nanomechanical resonator arrays," *J. Appl. Phys*, vol. 109. no. 10,p.104903, May. 2011

[7] H. Zhang, B. Li, W. Yuan, M. Kraft and H. Chang, "An Acceleration Sensing Method Based on the Mode Localization of Weakly Coupled Resonators," *J. Microelectromechanical Syst.*, vol. 25. no. 2,pp. 286-296, Apr. 2016.

[8] C. Zhao, M. Pandit, B. Sun, G. Sobreviela, X. Zou and A. A. Seshia, "A Closed-Loop Readout Configuration for Mode-Localized Resonant MEMS Sensors," in *J. Microelectromechanical Syst.*, vol. 26, no. 3, pp. 501-503, Jun. 2017.

[9] C. Zhao, G. .S Wood, S. H. Pu, and M. Kraft, "A Feasibility Study for a Self-oscillating Loop for a Three Degree-of-Freedom Coupled MEMS Resonator Force Sensor," in *Procedia Eng.*, vol. 120, pp. 887-891, 2015.

[10] C. Zhao, G. .S Wood, J. Xie, H. Chang, S. H. Pu and M. Kraft, "A Three Degree-of-Freedom Weakly Coupled Resonator Sensor With Enhanced Stiffness Sensitivity," in *J. Microelectromechanical Syst.*, vol. 25, no. 1, pp. 38-51, Feb. 2016.